CHAPTER 4

CONTINUOUS FOAMING PROCESS FOR LOW DENSITY AND FINE-CELLED PP FOAM MANUFACTURING

4.1 Introduction

This research studied the production of low density and fine-celled PP foams by using a tandem extrusion system together with an investigation of the processing parameters and the composition used in the system. The conceptual design and the functional detail of the tandem extrusion system were explained in 2.2.6 of Chapter 2. Unlike the processing with the solid-state batch foaming process, the understanding of the relation between the mechanism of expansion of the final foamed volume and the processing condition is very important in the continuous foaming process, because it is not easy to maintain the shape and the volume expansion ratio of the final PP foam by using the extrusion foaming process. Moreover, the difficulty of using PP material in the continuous process is related to the weak melt strength during the process. Therefore, the modification of the new material is an alternative way to obtain the required foam products. In the extrusion foaming process, nucleation or formation of expandable bubbles begins within the polymer melt that has been supersaturated with the blowing agent. Once a bubble reaches a critical size, it continues to grow as the blowing agent rapidly diffuses into it. This growth will continue until the bubble stabilizes or rupture [125]. When cell nucleation takes place in the extrusion foaming die, the cells grow and the foam density decrease (i.e., void fraction increases) as the available blowing agent

molecules diffuse into the cells. In general, cell growth is affected primarily by the time allocated for cells growth, the temperature of the system, the state of supersaturation, the hydrostatic pressure of stress applied to the polymer matrix, and the viscoelastic properties of the polymer/gas solution [12, 126]. Since foam products made from linear PPs usually have limited expansion capabilities due to their weak melt strength, material modification and new resin developments have been actively researched in order to improve the foamability. In particular, to achieve the desirable foam characteristics the utilizing of optimum die geometry is very important on the volume expansion and cell nucleation behavior of PP foams. Therefore, a feasible filament die was selected based on the results of Lee *et al.* experiment [16] for using in this research.

The purpose of die design is to actively control the geometries of the filamentary die, i.e. the die diameter and the die length, so that they will present the effects of different die pressures and different pressure drop rates on the final foam structure. The theoretical calculation of die pressure and pressure drop rate can be described by the power law as the experiment of Xu *et al*. [125].

Xu *et al*. [125] assumed that the viscosity of the polymer/gas solution is shear-rate dependent and could be described by the "power law" in the flow through a tube [35]. Therefore, the three interchangeable groups of 9 dies with the same pressure or the same pressure drop rate could be designed using the "power law" [125]. The pressure drop, P_{die}, over the length of a nozzle for a non-Newtonian fluid in a fully developed flow can be expressed as Equation 4.1 [125].

$$P_{die} = 2p\frac{L_{die}}{R_{die}^{3q+1}}\left[\left(3+\frac{1}{q}\right)\frac{Q}{\pi}\right]^{q} \qquad (4.1)$$

Where P_{die} is the pressure drop across the nozzle; Q is the volume flow rate of the polymer/gas solution; p and q are characteristics of the material; L_{die} is the length of the nozzle; and R_{die} is the radius of the nozzle. In order to derive the pressure-drop rate of the die, the residence time should be determined. The average residence time, $t_{residence}$, of the flowing polymer/gas solution in the nozzle can be expressed as Equation 4.2 [125].

$$t_{residence} \approx \frac{L_{die}}{v_{avg}} = \frac{L_{die}}{Q \big/ \pi R_{die}^2} = \frac{\pi R_{die}^2 L_{die}}{Q} \tag{4.2}$$

Therefore, the pressure-drop rate, dp/dt can be estimated as the following equation;

$$\frac{dp}{dt} \approx \frac{P_{die}}{t_{residence}} = -2p\left(3 + \left(\frac{1}{q}\right)\right)^q \left(\frac{Q}{\pi R_{die}^2}\right)^{q+1} \tag{4.3}$$

The power law parameters were determined from standard measurement using a cone-plate rheometer at 190 °C. The best fitting data, in a least square sense, are; p = 2100 N-s$^{0.51}$/m^2 and q = 0.51. The flow rate was chosen at 13 g/min, a typical value for extrusion studied. The calculated geometries of 8 filamentary dies are illustrated in Figure 4.1 [16] and summarized in Table 4.1 [16]. Among the same pressure dies; dies 1, 4, and 7 (i.e., 6.9 MPa), dies 2, 5, and 8 (i.e., 13.8 MPa), and dies 3 and 6 (i.e., 20.7 MPa), some variations of die pressure were observed. However, the die pressure could be distinctively differentiated among different pressure dies. It was expected that the dies in each die group (e.g., dies 1, 2, and 3) have the same pressure drop rate because of the same diameter [125]. The initially designed dies have to be calibrated for actual experiments, mainly due to two reasons.

First, the viscosity data from a cone-plate rheometer deviates from the one encountered during actual extrusion, because both die pressure (several thousand psi, as against atmospheric pressure for standard rheological tests) and non-uniform shear rates inside the die affect the viscosity. Second, the residence time used in the calculation is only an average value. The calibrated die geometries are shown in Table 4.1 [16]. The geometrical parameters of the eight die geometries with the varied pressure drop levels (6.9 MPa, 13.8 MPa, and 20.7 MPa) were recalculated. It should be noted that at the same time, three different pressure drop rates were chosen at 155 MPa/s, 48 MPa/s, and 7.2 MPa/s compared to the experiment of Xu *et al*. [125].

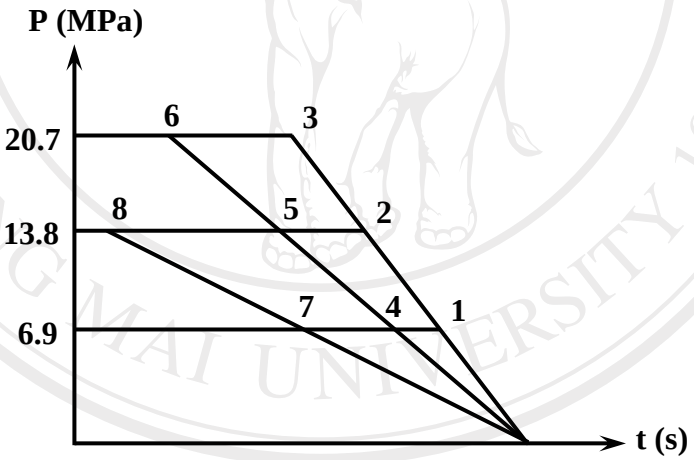

Figure 4.1 Targeted pressure drop and pressure drop rate for the 8 filamentary dies for HMS PP [16].

Table 4.1 Calculated geometry, residence time, and pressure drop rate of the dies for HMS PP [16].

Die Group	Die No.	Pressure Drop Level, MPa (psi)	Die Diameter, mm (inch)	Die Length, mm (inch)	Average Residence Time, ms	Pressure Drop Rate, MPa/s
Group 1	Die 1	6.9 (1000)	0.940 (0.037)	12.79 (0.50)	44.4	155.0
	Die 2	13.8 (2000)	0.940 (0.037)	25.70 (1.01)	89.2	155.0
	Die 3	20.7 (3000)	0.940 (0.037)	38.61 (1.52)	134.0	155.0
Group 2	Die 4	6.9 (1000)	1.219 (0.048)	24.73 (0.97)	144.0	48.0
	Die 5	13.8 (2000)	1.219 (0.048)	49.70 (1.96)	290.0	48.0
	Die 6	20.7 (3000)	1.219 (0.048)	74.68 (2.94)	435.0	48.0
Group 3	Die 7	6.9 (1000)	1.854 (0.073)	71.30 (2.81)	962.0	7.2
	Die 8	13.8 (2000)	1.854 (0.073)	143.3 (5.64)	1930.0	7.2

Since the material used of Lee *et al*. [16] experiment was different from that of Xu *et al*. [125], the geometrical parameters of the dies should be recalculated and the calibrated geometries of the die for HMS PP were shown in Table 4.2 [16]. It should be noted that at the same time, three different pressure drop rates were chosen at 155 MPa/s, 48 MPa/s, and 7.2 MPa/s compared to Xu *et al*. [125]. The chosen pressure and pressure drop rates are lower such that the possibility of achieving a high expansion ratio at a lower cell density can be studied.

Table 4.2 Re-calibrated geometries of the dies for HMS PP [16].

Die Group	Die No.	Die Diameter, mm (inch)	Die Length, mm (inch)
Group 1	Die 1	0.940 (0.037)	7.50 (0.295)
	Die 2	0.940 (0.037)	17.03 (0.670)
	Die 3	0.940 (0.037)	26.10 (1.028)
Group 2	Die 4	1.219 (0.048)	14.64 (0.576)
	Die 5	1.219 (0.048)	29.36 (1.156)
	Die 6	1.219 (0.048)	44.55 (1.754)
Group 3	Die 7	1.854 (0.073)	48.21 (1.898)
	Die 8	1.854 (0.073)	121.07 (4.767)

As the experiment of Lee *et al*. [16], the volume expansion and nucleation behaviors of HMS-branched PP foams with various die geometries and processing parameters were investigated as shown in Figure 4.2-4.3 [16]. The volume expansion ratios and cell densities were a function of the die temperature for all eight dies. As mentioned in the previous part, the same diameter of the die should have the same pressure drop rate even the die pressure could be distinctively differentiated among different pressure dies [127]. The influence of processing conditions on the foaming behaviors was discussed as following.

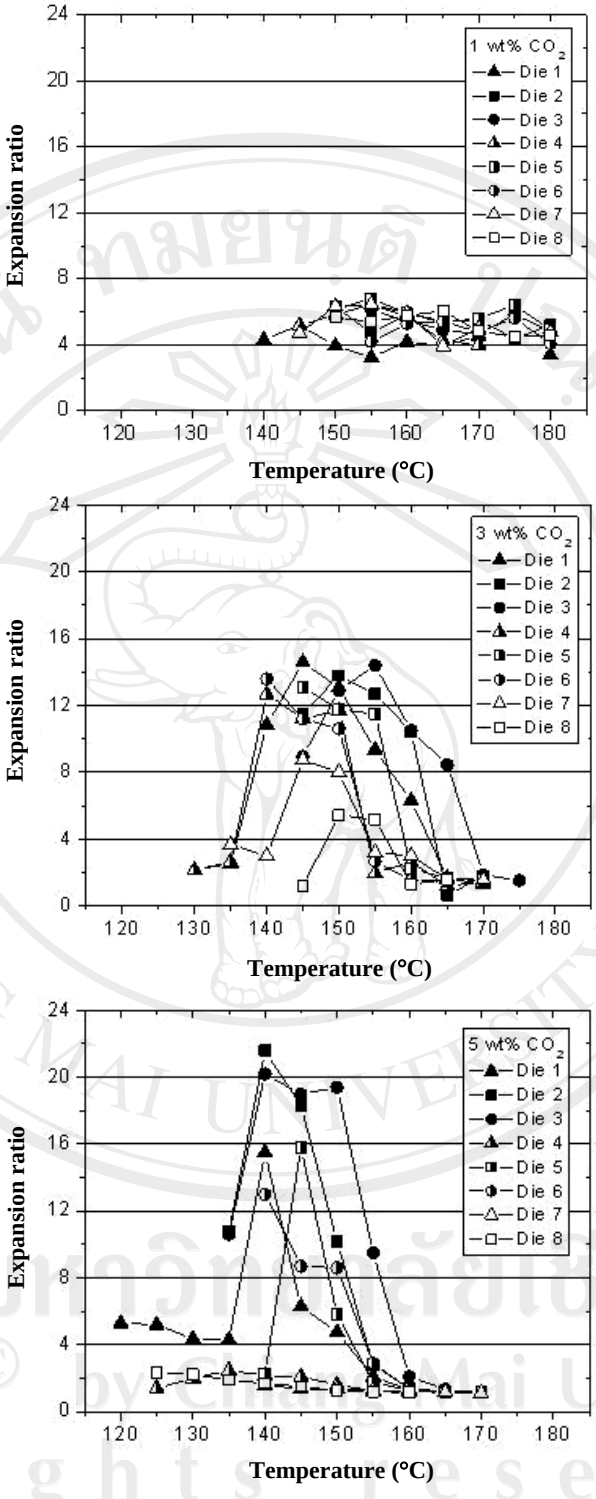

Figure 4.2 Expansion ratios versus die pressure at; (a) 1 wt% of CO_2, (b) 3 wt% of CO_2, and (c) 5 wt% of CO_2, respectively [16].

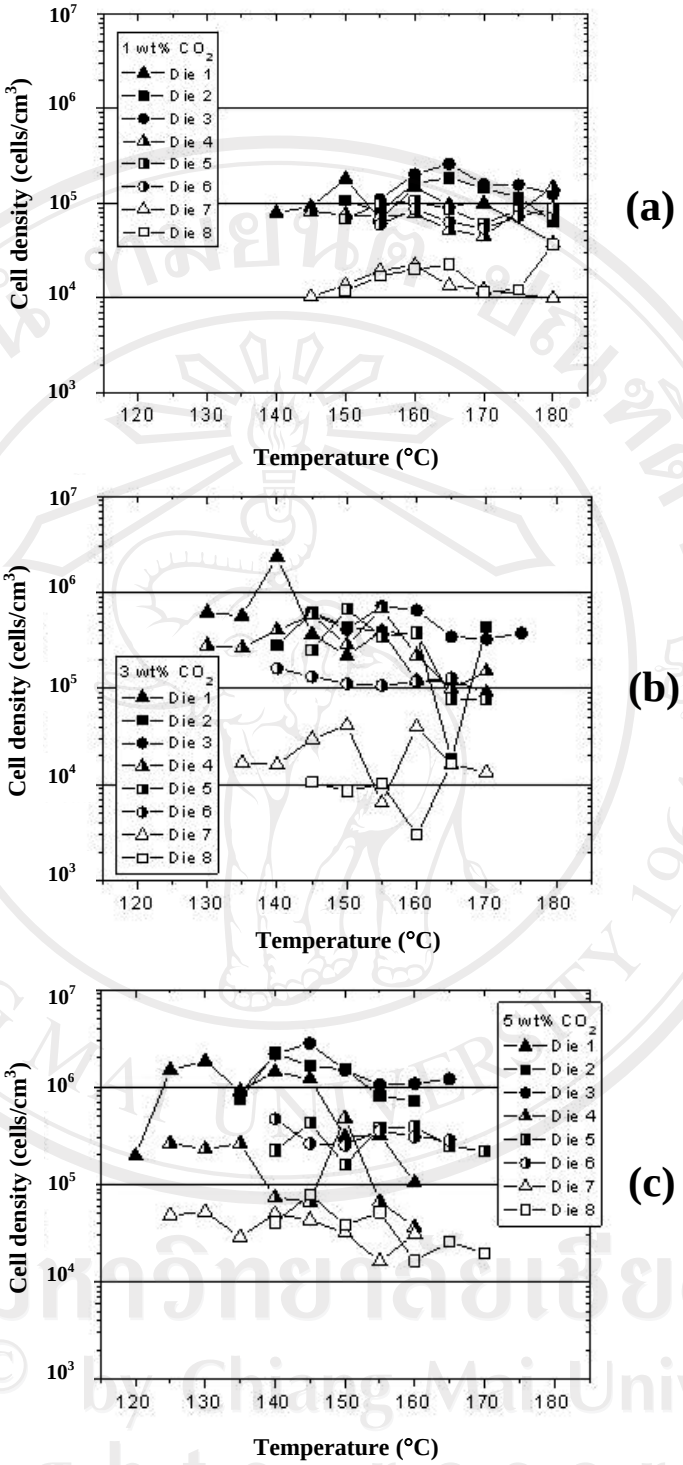

Figure 4.3 Cell densities versus die pressures at; (a) 1 wt% of CO_2, (b) 3 wt% of CO_2, and (c) 5 wt% of CO_2, respectively [16].

The expansion ratios of PP foams blown with CO_2 exhibited the mountain-shaped curves as shown in Figure 4.2 (b)-(c), indicating the existence of the optimum temperature range for maximum expansion. The expansion ratio was constrained by two major mechanisms; the serve loss of CO_2 through the foam skin at high temperature and the crystallization of the polymer matrix at low temperatures as described in Chapter 2. However, the typical mountain-shaped expansion curves were not observed for 1 wt% of CO_2 experiments (Figure 4.2 (a)) due to the lack of gas in the polymer matrix to be utilized for foam expansion. Consequently, the maximum expansion ratios were only about 7 fold. It should be noted that the expansion ratios from low pressure die experiments (dies 1, 4, and 7) with 5 wt% of CO_2 were significantly lower than those of higher pressure die experiments. This is because a large amount of undissolved gas pockets formed in the die land ($P_{die} < P_{solubility}$). It is believed that this undissolved CO_2 contributed significantly to the collapse of expansion ratios [16]. Xu and Park [128] claimed that the pressure would not affect the premature cell-growth time when the die radius (i.e., the pressure-drop rate) is the same. Moreover, the degree of premature cell growth would not be a function of the pressure since the cell density would be insensitive to the pressure. This means that within the same die groups (or same pressure drop rate), the nucleation and expansion behaviors should be almost similar as long as the die pressure are above the solubility pressure of CO_2 at the given conditions. Figure 4.2 (b)-(c) show that a high pressure drop rate is favorable to get a large expansion ratio for the PP/CO_2 system. As the pressure drop rate decreased from 155 to 7.2 MPa/s (i.e., group 1 to group 3), the expansion ratio decreased. The effect of pressure drop rate became more dramatic as CO_2 content increased. In Figure 4.2 (c), three distinctive groups of expansion ratios

(correspondent to each die group) were observed except for low pressure die cases (i.e., die 1 and 4). The low expansion ratios of die 1 and 4 experiments were due to undissolved gas pocket in the die land as mentioned in the earlier section. Two major factors have contributed to the final expansion ratio with respect to the pressure drop rate; (1) premature cell growth amount, and (2) the number of cell layers in the cross-section of the extruded. According to Xu and Park [128], the premature cell growth amount using the highest pressure drop rate dies are the smallest due to the decreased premature cell growth time. They found that the maximum expansion ratio obtained from each die decreased as the premature cell growth amount increased. The other factor which may have affected the final expansion ratio was the number of cell layers in the cross-section of the extrudate. As a cell density increased with a high pressure drop rate, the number of cell layers of the extrudate also increased. Moreover, an increase in the expansion ratio of extruded foams with a high cell density due to the localized gas loss in the foam surface area can be applicable to explain this PP/CO_2 experiments.

As the results of this experiment, it could be concluded that first, the typical mountain-shaped curve which was found in 3 and 5 wt% of CO_2 experiments, indicated that gas loss and stiffening of the melt were two governing mechanisms of expansion. The expansion ratios of 1 wt% of CO_2 experiments were only 4 to 7 folds within the whole processing temperature range. The effect of die pressure (within the same die group) on cell nucleation and expansion behavior seemed to be negligible as long as the die pressure was above the solubility pressure of CO_2. Although, the nucleation and expansion behavior showed little difference within the same die group but both cell density and volume expansion ratio increased as the die pressure drop

rate increased. Figure 4.3 demonstrates that the cell densities within the same die group show little difference, supporting the previous arguments. Only exceptions were the low die pressure experiments (die 1, 4, and 7) for the same reason described in the earlier section. As the results in Figure 4.3, the cell density was insensitive to the die temperature but it was found to be a very sensitive function of the die-pressure drop rate at all CO_2 contents. As CO_2 content increased from 1 to 5 wt%, the overall cell-population densities steadily increased for all eight dies. Therefore, this information could be conducted as a basic approach to find the feasible filamentary die for producing low-density and fine-celled PP foams using the tandem extrusion foaming process as indicated in the following section.

4.2 Manufacturing of low-density and fine-celled PP foams

In order to obtain the PP foam with the desired cell density and volume expansion ratio, the investigation of the effect of die dimension on the final foams was evaluated through of the processing parameters (i.e., die temperature, die pressure, and pressure drop rate at the exiting die). The results of the experiments were discussed and summarized as the previous section. In order to get the fundamental die design for production, the PP foams with the desired foamed properties in the previous experiment has been applied to use as the approach to design a die for the production of low-density and fine-celled PP foams.

For this section, the manufacturing of the foaming behavior of recyclable HMS branched PP with CO_2 as a blowing agent has also been studied using a tandem foaming extruder system. The effects of CO_2 and nucleating agent contents on the final foam characteristics have been thoroughly investigated. Low density (i.e., 12-14

fold) and fine-celled (i.e., 10^7-10^9 cells/cm^3) PP foams were successfully produced using a small amount of talc (i.e., 0.8 wt%) and 5 wt% CO_2. The detail of the experiment will be discussed as the following sections.

This experiment was done by the encouragement of the recent consumption of raw plastic material which has significantly increased worldwide, and also the automotive manufacturing industries are attempting to reduce the quantity of non-recyclable plastic scraps which must be disposed of in landfills [129]. Therefore, the action of the plastic manufacturing has shifted to potentially recyclable materials such as non-crosslinked polypropylene (PP); the potential polymer for the bumper system, instrument panel, seat, and other interior trim components. Therefore, it is worthwhile to study the processability of recyclable PP for foaming applications. As the previous parts that explain about the characteristics of foams or cellular polymers which provide the unique properties that enable foamed plastics to be effectively used for various industrial applications such as automotive and packaging [2, 5, 130]. Moreover, these foamed characteristics also influence the final properties of the foams; such as low density foams (i.e., less than 64 kg/m^3) are primarily used for load bearing application [2] and the foams with very fine celled and uniform cell distribution exhibit better mechanical properties such as toughness [45], impact strength [10, 80, 100, 131], and tensile strength [107], etc. Fine-celled foams are characterized by a cell size smaller than 100 μm and a cell density larger than 10^6 cells/cm^3. These foamed materials can reduce the weight significantly and thereby lower the material cost [77, 130, 132].

The process of making fine-celled polymers has been developed based on a thermodynamic instability which is induced by rapidly dropping the solubility of gas

in the polymer melt to drive cell nucleation and cell growth to produce foam expansion. The continuous foaming process is an alternative method to overcome the limitation of a batch-foaming process. In this continuous foaming method, a much shorter time was needed to saturate the polymer with gas. When polymer was melted in the extrusion barrel, a metered amount of gas was delivered to the polymer melt. Injected gas diffused into the polymer matrix at a much higher rate because of convective diffusion induced in the extrusion barrel at elevated temperatures. The formation of a uniform solution of polymer and gas is essential in fine-celled foam processing since undissolved gas packet can generate nucleation is promoted using a rapid pressure drop rate nucleating shaping at the die exit [45, 91, 93, 109].

Although, polypropylene has the outstanding properties such as higher rigidity, higher strength, higher service temperature range and good temperature stability compared to other polyolefins but linear PP has not been used much in the foaming industry due to their weak melt strength [7, 132-139]. Because of the weakness, cell walls separating and cells or bubbles may not be strong enough to resist the extensional force and may rupture very easily during foaming. This results in severe cell coalescence in the final PP foam structure. When cells coalesce, not only are cell density and cell size uniformity deteriorated, but the volume expansion ratio is also greatly decreased due to accelerated gas loss through opened cell walls. Therefore, using a long-chain branched resin is essential for producing low density fine-celled PP foams [7, 132-133, 136-137].

It is well known that the melt strength of a polymer can be enhanced by branching [7, 132-139], crosslinking [13, 80], controlling of processing temperature [33-35], controlling of molecular weight and molecular weight distribution [136, 141-

142], and blending of polymers [135, 142]. For example, in order to improve foamability, crosslinking of the polymer matrix can be induced to generate a partly solidified state which may contribute to strain-hardening [45, 136]. Therefore, the easiest feasible method for promoting large expansion by increasing the melt strength of PP foams is to use branched PP materials [7, 134-139]. Using a long-chain branched PP with high melt strength and high-melt extensibility, cell coalescence is more effectively prevented compared to linear PP [7, 13, 135-139]. The most important characteristics of a long-chain branched PP for foaming are the high-melt-strength (HMS) properties, which can exhibit high elastic response, two-step viscosity at low frequencies (shear rates), and various relaxation processes in the nonlinear relaxation modulus. Therefore, introducing long chains may be the exceptional method to obtain excellent melt properties without any disadvantages such as decomposition, aggravation of physical properties, etc. In the foaming process of HMS PP, cell density and volume expansion can be enhanced due to a lower degree of cell coalescence in the cell growth stage [7, 15]. Therefore, HMS branched PP material has been regarded as a good candidate for producing low-density, fine-celled foams, Furthermore, HMS PP can be recycled after processing.

Due to an increasing of safety and environmental concerns over the use of the conventional flammable, volatile organic hydrocarbons, attention has shifted to using the environmentally friendly gases such as carbon dioxide (CO_2) and nitrogen (N_2) [86]. Organic hydrocarbons such as butane, pentane, etc provide a lower the maximum achievable expansion ratio. It is known that CO_2 has been effectively used for producing fine-celled or microcellular foams with a small amount of nucleating agent such as talc [17, 77, 87, 144].

Normally, nucleating agents are finely powdered to serve as solid surfaces for heterogeneous cell nucleation, and they remain solid or thermally stable during the foaming process. The condition for heterogeneous nucleation depends on the surface geometry and surface energies (between solid-liquid, solid-gas, and liquid-gas) [1]. If the free energy for gas cluster formation on the surface of a nucleating agent is less than for homogeneous nucleation in the polymer melt, heterogeneous nucleation on the solid phase will occur. It is expected that nucleating agents play an important role in determining the cellular structure of thermoplastic foams. Unless a thermodynamic instability via a rapid solubility drop is utilized to promote a large number of nuclei. Final foam structure is usually unacceptable without the addition of a nucleating agent; namely, the bubble size is too large and cell density is too small. In the PP foaming process, the addition of a nucleating agent was essential in achieving a good nucleus density. Moreover, it is expected that the high processing pressure and high pressure drop rate required to producing large cell density can be lowered by using a nucleating agent. It would be beneficial if the high nuclear density could be obtained at a lower pressure and pressure drop rate by adding a small amount of nucleating agent [77, 87, 144].

4.3 Research objective

This study was to produce fine-celled (i.e., cell size smaller than 300 μm) with the cell density in the range of 10^6-10^9 cells/cm^3 and low density (i.e., in the range of 4-30 folds) foams using the tandem foaming extruder system and environmentally benign CO_2. The foaming behaviors of HMS PP foams have been investigated. Cell nucleation and expansion behaviors of extruded PP with various

contents of CO_2 and nucleating agent were studied. In addition, the effects of processing conditions on the final foam morphologies have also been examined through the experiments.

4.4 Experimental

4.4.1 Materials

The plastic material used in this study was a high-melt-strength (HMS) branched PP resin (Honam SMS-514) supplied by Honam Petrochemical Corporation Company. The blowing agent was CO_2 with 99.5% purity (supplied by BOC Gas Co.). The nucleating agent used for creating the voids in the polymer was mean particle size 7 μm of talc.

4.4.2 Investigation of polypropylene (Honam SMS-514) properties

The melt flow index of the material was processed by Melt Flow Indexer (Dynisco Polymer Test) based on the ASTM D1238 [145]. In the process, the polymer pellets was allowed to extrude through the heating chamber which heated up to 230 °C using 2.16 kg of load. The weight (g) of extruded part at the collected time was measured and then it was converted into g/10 min. The test was done for 3 times for this material and the resulting MFI was shown in Table 4.3.

In addition, differential scanning calorimeter (DSC; DSC 2910, TA instrument) was used to analyze the thermal history of Honam SMS-514. The typical weight 3-5 mg of polymer was processed under N_2 atmosphere. The polymer was heated up in the temperature range of 25-230 °C at 10 °C/min in order to identify the melting temperature (T_m) and crystallinity. After that the sample was cooled down

from 230 °C to the initial temperature at 10 °C/min in order to investigate the crystallization temperature (T_c) of the polymer. The DSC thermogram of this polymer is shown Figure 4.4. The crystalline fraction was calculated based on that of the completely crystallized PP polymer (209 J/g) [116].

Table 4.3 Melt flow index of Honam SMS-514 at 230 °C and 2.16 kg.

Test No.	Weight (g)	Flow time (min)	MFI (g/10 min)
1	0.5057	2.04	2.478
2	0.5136	2.08	2.469
3	0.5147	2.05	2.511
		Average	2.486 ± 0.022

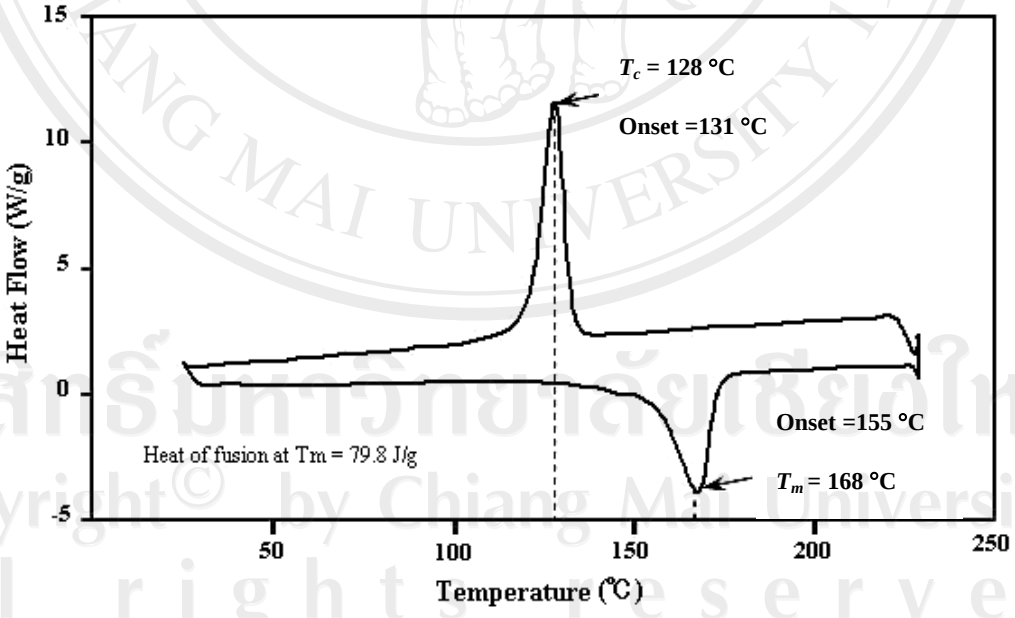

Figure 4.4 DSC thermogram of HMS-branched PP resin at the heating and cooling rate of 10 °C/min.

4.4.3 Foaming procedure

1) Sample preparation

The HMS branched PP resin was mechanically mixed with a different concentrations of talc particles (i.e., 0.8 wt%, 1.6 wt%, and 2.4 wt%). For example, if 0.8 wt% of talc content is desired, 960 g of branched PP resin is mixed with 40 g of 20 wt% talc-filled PP resin. Then the 1000 g of polymer blend will have 0.8 wt% talc embedded in it. The sample without talc was also performed. Further, these mixtures will be embedded with different contents of CO_2 gas in the foaming process using the extruder foaming system as following.

2) Experimental setup

After investigation of the effect of die geometry on the foamability of final PP foams, an optimum feasible filamentary die was selected to use as a die to produce the low-density, fine-celled PP foams. The process of this experiment was performed using the tandem foaming extrusion system. This machine consists of 5 hp extruder driver with a speed control gearbox (Brabender; Prep center), a first 3/4″ extruder (Brabender; 05-25-000) with a mixing screw, a second 1.5″ extruder with a built-in 15 hp variable speed drive unit (Kilon; Kn-150), a positive displacement pump for injecting the blowing agent into the polymer melt, a gear pump (Senith PEP-II 1.2 cc/rev), a heat exchanger (for cooling the polymer melt) which contains homogenizing static mixers, a filament die with various length/diameter (L/D) ratios, and a cooling sleeve for precise control of die temperature. The first extruder is used for plasticizing polymer resin. The second extruder provides mixing and initial cooling for the polymer melt. The gear pump controls the polymer melt flow rate,

independent of temperature and pressure changes. The heat exchanger provides further cooling for the polymer melt to suppress cell coalescence. Shaping and foaming are done in the filament die. The foaming system was set as a part of experimental setup of the investigation of die geometries as described in 4.2.3. The die 3 (L/D = 0.940 mm/26.1 mm) was selected to use as a filamentary die but the length of the die was shortening to have 21.84 mm (0.86″) in length but the diameter was remain as 0.94 mm (0.037″) in order to obtain the optimum pressure drop level for accomplishment of the desired PP foam properties. Therefore, the final filamentary die with a length/diameter (L/D) ratio of 21.84 mm (0.86″)/0.94 mm (0.037″) was applied in the system.

3) Experimental procedure

The PP pellets and the mixed-PP pellets with various talc contents (0.8 wt%, 1.6 wt%, and 2.4 wt%) were first fed into the barrel through a hopper and were completely melted by a screw motion. A metered amount of blowing agent was then injected into the extrusion barrel by a positive displacement pump at a given weight percentage with the polymer stream. When gas was injected into the barrel, the remaining section of the first screw and second screw generated shear fields to completely dissolve gas in the polymer melt via convective diffusion. The single-phase polymer/gas solution went through the gear pump and was fed into the heat exchanger where it was cooled to the desired temperature. The cooled polymer/gas solution entered the die, and foaming occurred as pressure decreased near the die exit. While fixing all the other materials and processing parameters such as the screw speed, gear pump speed (i.e.,12 RPM), blowing agent content and barrel temperature

(i.e., 160 °C) in order to obtain a constant 12 g/min of gas/polymer mixture flow rate, the synchronized melt and die temperatures were lowered step by step, and samples were randomly collected at each set temperature only after the system reached the equilibrium state.

The foamed samples were randomly collected at each processing condition and were characterized by using a scanning electron microscope (SEM, JEOL JSM-6060) to evaluate the morphology. The samples were dipped in liquid nitrogen and then fractured to expose the cellular morphology, and then the fractured surface was sputter-coated with gold. The microstructure was investigated by SEM. The volume expansion ratio and cell density were the structural foam parameters measured. The expansion ratios of foams were examined by measuring the weight and volume of the sample.

4.4.4 Sample characterization

The expansion ratio of each sample was calculated as the ratio of bulk density of un-foamed sample to bulk density of foamed sample as shown in Equation 2.36 in Chapter 2. And according to ASTM D792, the density of the polymer pellets and PP foams could be calculated compared to the density of water at the experimental condition (22 °C; 0.9977 g/cm^3) as Equation 2.32 in Chapter 2. In addition, the basis of the ratio of the bulk density of foamed sample and un-foamed sample was used to calculate the void fraction described as Equation 2.34 in Chapter 2. The blowing agent efficiencies (η) were determined as Equation 4.4. The ideal volume expansion ratio was approximately calculated as Equation 2.33 or 2.34 in Chapter 2. The specific volume of CO_2 at the crystallization temperature of 128 °C

was 752.2 cm^3/g, and the specific volume of Honam SMS-514 resin at room temperature was 1.2408 cm^3/g, respectively [15].

$$\eta = \frac{v_a}{v_t} \tag{4.4}$$

For example, for the injected CO_2 amount of 1 wt%, the ideal volume expansion was estimated as follows [15]:

$$v_t = 1 + 0.01 \times \frac{752.2(cm^3/g)}{1.2408(cm^3/g)} \approx 7.0622$$

Cell density was calculated as Equation 2.35 in Chapter 2 and the determination of the average cell size could be indicated as Equation 2.37 in Chapter 2.

4.5 Results and discussion

4.5.1 Properties of PP pellets (Honam SMS-514)

After the melt flow index measurement, the average melt flow index of Honam SMS-514 was calculated and it was shown in Table 4.3. Its value is about 2.486 ± 0.022 g/10 min. As the result in Figure 4.4, the melting temperature of this polymer was 168 °C and crystallization temperature was 128 °C. The crystalline fraction was approximately 38% based on the crystalline fraction of the completely crystallized PP polymer. Consequently, the foamed samples of all studied processing condition were characterized. The effects of blowing agent contents (i.e., 1, 3, and 5 wt%), talc contents (i.e., 0.8, 1.6, and 2.4 wt%), and die temperatures (i.e., 140-180 °C) on the expansion ratio and cell nucleation behaviors of HMS PP was investigated to determine the process-morphology relationships. The effects of processing

parameters on expansion ratios and cell morphologies of the final foams were also discussed.

4.5.2 Pressure-temperature profile of foaming process

The pressure-temperature profiles during the foaming process of HMS-branched PP resin with various blowing agent contents and nucleating agent contents were shown in Figure 4.5. Figure 4.5 shows the decreasing of die pressure was a function of CO_2 contents. It was observed that the die pressure was decreased as the content of CO_2 increased from 1 wt% to 3 or 5 wt%. This was due to the effect of plasticization of the increased CO_2. It is known that the presence of high amount of blowing agent (gas) in the polymer melt, the added gas can act as a plasticizer to soft or swell the polymer [99]. Therefore, the reduction of the die pressure at the high amount of CO_2 could be observed. Moreover, when the foaming process was performed at the high die temperature, the die pressure was also decreased. At this condition, the pressure at the exiting die could be reduced due to the decreased viscosity of the polymer melt. However, the effect of talc content on the die pressure was not clearly seen at the same amount of CO_2.

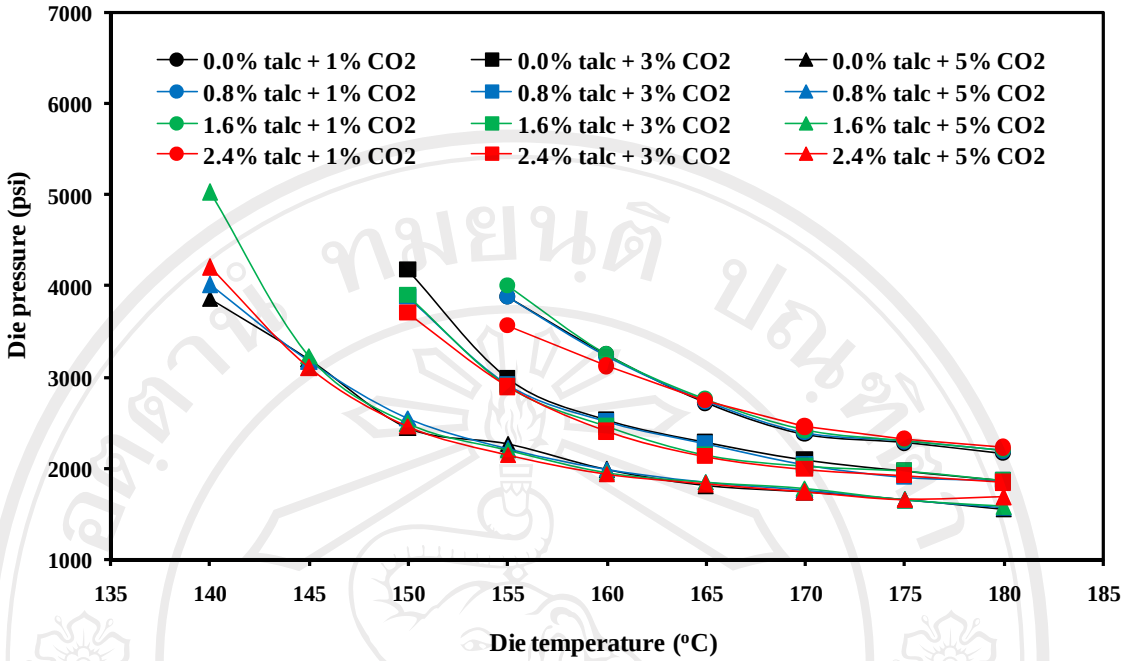

Figure 4.5 Pressure-temperature profile of foaming process of Honam SMS-514 with various processing conditions.

4.5.3 Densities of PP foams

The density of PP pellets was shown in Table 4.4.

Table 4.4 Density of PP pellets at 22 °C.

Experiment	1	2	3	4	5	6	Average
W_{air}	0.1499	0.1508	0.1566	0.1879	0.1704	0.1638	-
W_{water}	0.1837	0.1827	0.1822	0.2446	0.2318	0.1945	-
Density	0.8141	0.8235	0.8575	0.7664	0.7334	0.8402	0.8059±0.0469

Since the extruded samples processed under the different condition they were randomly selected to determine the density as the same manner as what was performed for PP pellets as the results in Table 4.5-4.8.

Table 4.5 The average density of PP foams with 1, 3, and 5 wt% of CO_2 without talc at various die temperatures.

Die temperature (°C)	Foam density at various CO_2 contents (wt%)		
	1%	3%	5%
180	0.3029	0.1900	0.5003
175	0.2730	0.1831	0.3699
170	0.2215	0.0939	0.2259
165	0.2013	0.1047	0.9220
160	0.2125	0.1012	0.1321
155	0.2066	0.1260	0.1047
150	n/a	0.4151	0.1010
145	n/a	0.0890	0.1122
140	n/a	0.1181	0.1895

Table 4.6 The average density of PP foams with 1, 3, and 5 wt% of CO_2 with 0.8 wt% of talc at various die temperatures.

Die temperature (°C)	Foam density at various CO_2 contents (wt%)		
	1%	3%	5%
180	0.1908	0.5343	0.5259
175	0.1635	0.3820	0.4403
170	0.1644	0.1499	0.3644
165	0.1804	0.1011	0.2721
160	0.2132	0.1018	0.1362
155	0.3980	0.1733	0.0705
150	n/a	0.2112	0.0593
145	n/a	n/a	0.0787
140	n/a	n/a	0.0990

n/a = not available

Table 4.7 The average density of PP foams with 1, 3, and 5 wt% of CO_2 with 1.6 wt% of talc at various die temperatures.

Die temperature (°C)	Foam density at various CO_2 contents (wt%)		
	1%	**3%**	**5%**
180	0.1838	0.5392	0.6062
175	0.1702	0.4281	0.5369
170	0.1894	0.2661	0.4410
165	0.1976	0.2020	0.2975
160	0.2127	0.1405	0.1519
155	0.4305	0.1483	0.0848
150	n/a	0.2646	0.0650
145	n/a	n/a	0.0836
140	n/a	n/a	0.1754

Table 4.8 The average density of PP foams with 1, 3, and 5 wt% of CO_2 with 2.4 wt% of talc at various die temperatures.

Die temperature (°C)	Foam density at various CO_2 contents (wt%)		
	1%	**3%**	**5%**
180	0.2010	0.5521	0.5229
175	0.1898	0.4131	0.4970
170	0.1943	0.3131	0.4349
165	0.2081	0.1800	0.3037
160	0.3015	0.1186	0.1883
155	0.4350	0.1369	0.0822
150	n/a	0.1786	0.0615
145	n/a	n/a	0.0895
140	n/a	n/a	0.1431

n/a = not available

After that the volume expansion ratios of the PP foams were calculated based on the density results in Table 4.6-4.8 compared to that of PP pellets. The relationship of volume expansion ratios and die temperature, and the relationship between the maximum volume expansion ratios versus CO_2 and talc contents were shown in Figure 4.6-4.9 and 4.10, respectively.

4.5.4 Effects of processing parameters on the volume expansion ratio

1) Die temperature

Figure 4.6-4.9 showed the expansion ratios versus die temperature of foams with various CO_2 contents and talc contents. The typical mountain shaped curves [17, 131] were observed, which clearly appeared when the CO_2 content was higher than 1 wt% for all talc contents. It can be explained that expansion behaviors were governed by gas loss at high temperatures because of high gas diffusivity. When the melt temperature was too high, most of the gas escaped through the hot skin layer of foam during the initial stages of expansion. This led to the presence of only a small amount of residual gas inside the cells, resulting in insufficient gas pressure for foam expansion (i.e., the force exerted by gas pressure was insufficient to overcome the melt strength). Therefore, the final expansion ratio was low at high temperatures. In addition, at low temperatures, expansion behaviors were governed by the stiffness of PP melt; the melt strength of PP due to crystallization is higher than that of gas pressure entrapped inside the cells. According to the result of thermal history analysis, polymer started to crystallize at 155 °C, as shown in Figure 4.4. Therefore, foaming the PP with a small amount of CO_2 (i.e., 1 and 3 wt%) near the onset crystallization temperature was very challenging; the bubbles could not grow due to stiffened cell

walls. This also resulted in low expansion ratios [17, 131]. For 5 wt% CO_2 experiments, processing at much lower temperature was possible due to the plasticizing effect of residual gas inside the polymer melt. Consequently, the optimum temperature for a maximum expansion ratio was shifted to a lower temperature for all talc content experiments.

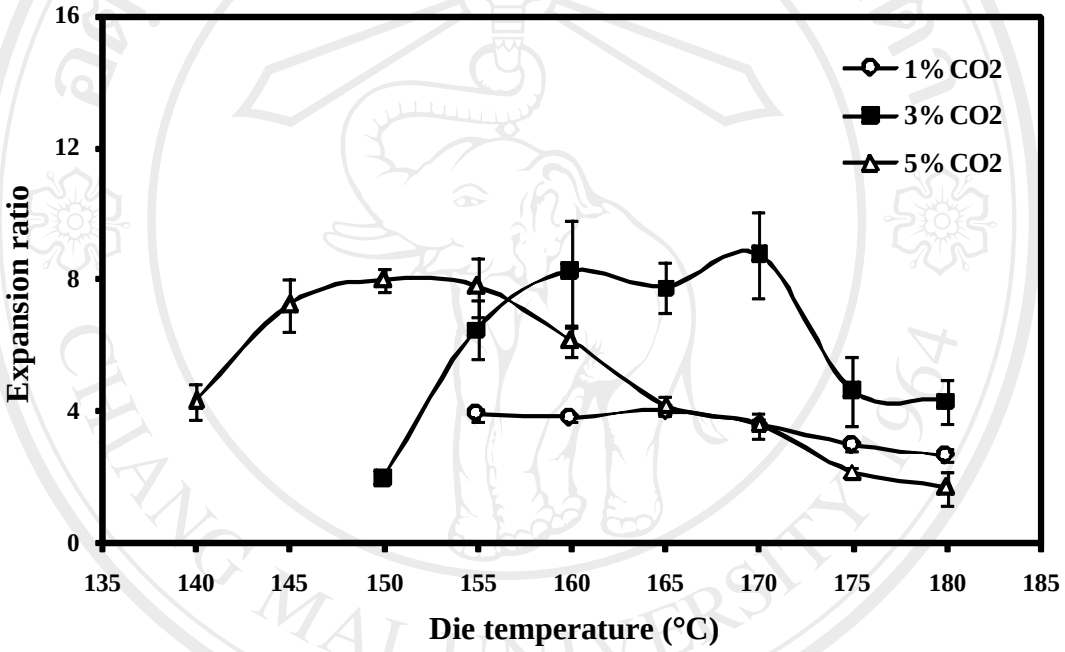

Figure 4.6 Volume expansion ratios of PP foams with 1, 3, and 5 wt% of CO_2 without talc at various die temperatures.

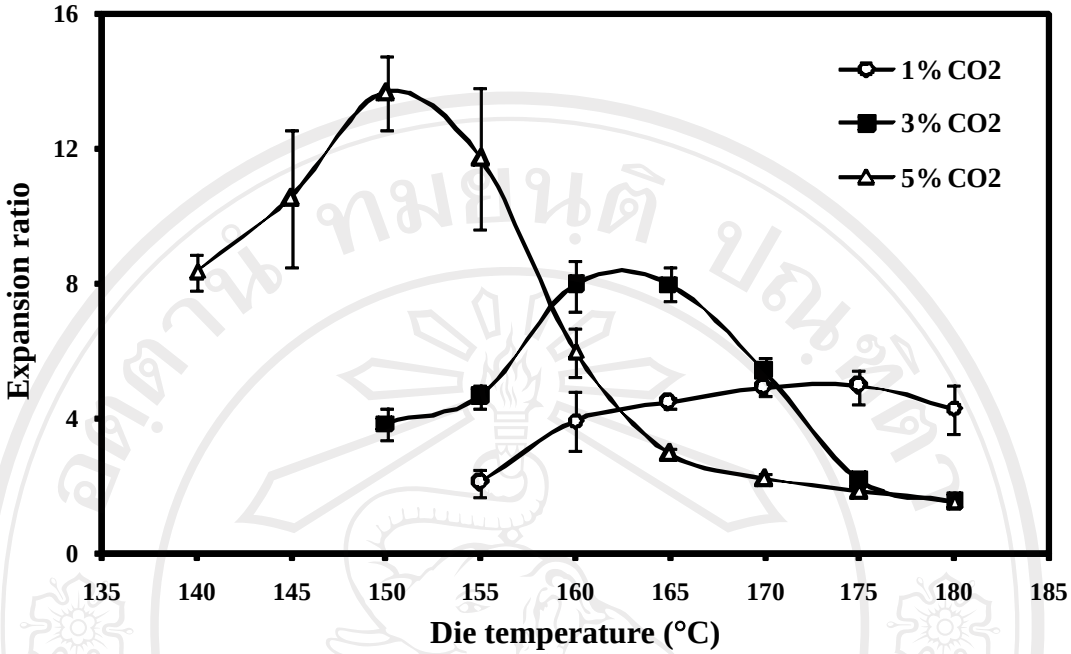

Figure 4.7 Volume expansion ratios of PP foams with 1, 3, and 5 wt% of CO_2 with 0.8 wt% of talc at various die temperatures.

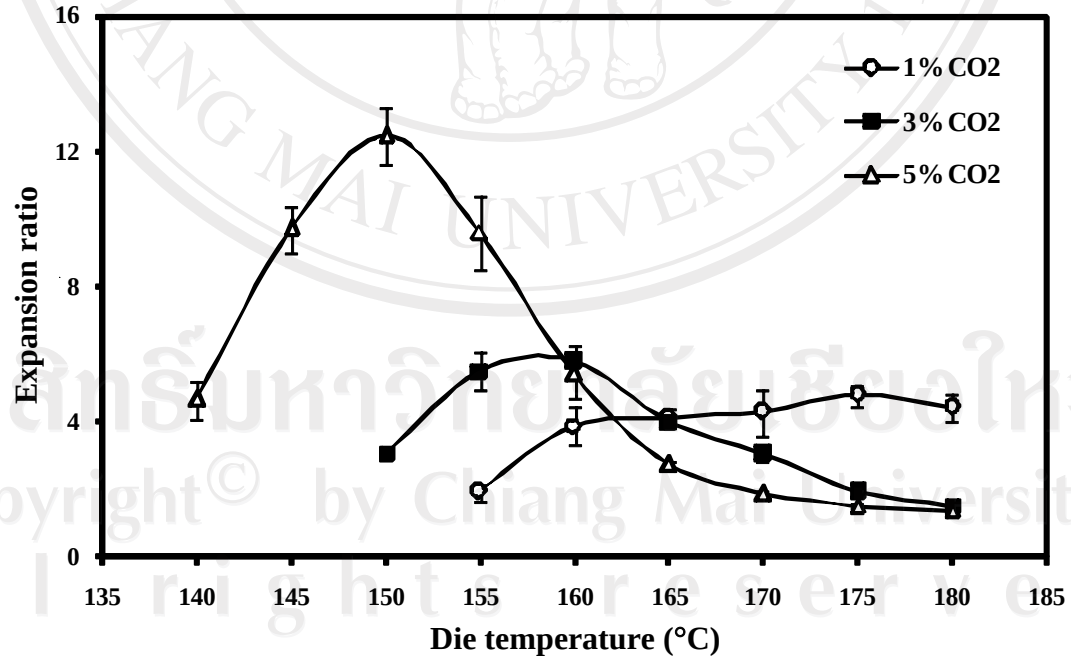

Figure 4.8 Volume expansion ratios of PP foams with 1, 3, and 5 wt% of CO_2 with 1.6 wt% of talc at various die temperatures.

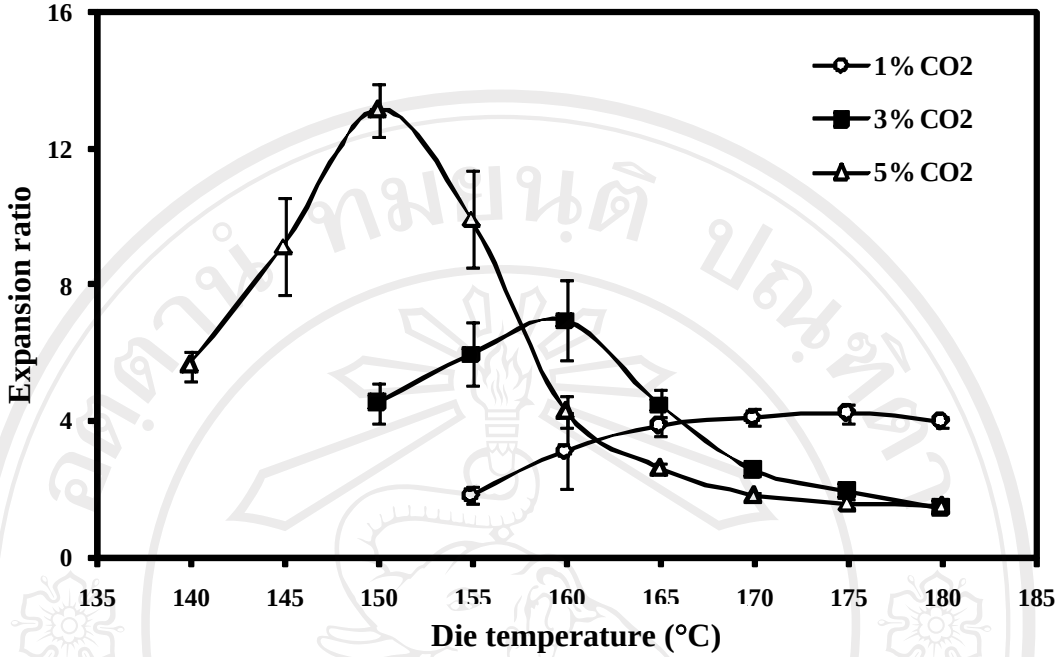

Figure 4.9 Volume expansion ratios of PP foams with 1, 3, and 5 wt% of CO_2 with 2.4 wt% of talc at various die temperatures.

2) Blowing agent content

The optimum temperature shifted to lower temperatures when the amount of CO_2 was increased from 1 to 5 wt%. This shifted in optimum temperature was due to the plasticizing effect of increased CO_2 content in the polymer matrix. Moreover, die pressure decreased as CO_2 content was increased, as shown in Figure 4.5. The significant dropped in processing pressure as the amount of injected CO_2 increased was due to the effect of the viscosity drop of molten polymer with CO_2. It was observed that the effect on expansion behavior of foams was not clear when foaming with a low content of CO_2 (1 wt%) for all talc contents (Figure 4.6-4.9). The maximum expansion ratios were only 4-6 folds over the entire temperature range. As CO_2 content was increased to 3-5 wt%, mountain shaped curves were observed, and

expansion ratios increased as CO_2 contents increased. The maximum expansion ratios up to 12-14 folds were successfully obtained at 5 wt% CO_2 with a small amount of talc (i.e., 0.8-2.4 wt%), as shown in Figure 4.10-4.11.

3) Nucleating agent content

When foaming without a nucleating agent, the volume expansion ratios were only 2-9 folds at all CO_2 contents (i.e., 1-5 wt%). Therefore, adding talc in the process could enhance volume expansion. Consequently, maximum expansion ratios of up to 14 folds were achieved by using 0.8 wt% talc with 5 wt% CO_2. While increasing the concentration of talc (i.e., > 0.8 wt%), the maximum expansion ratio was slightly decreased as shown in Figure 4.11. It seemed that too much talc worked negatively to enhance the expansion of foamed samples. It is believed that too much talc would increase the open cell fraction and thereby increase foam density. The reason did not seem to be clear, but it would be one of the following two reasons. First, higher talc content resulted in a higher cell density (and thereby a thinner cell wall). The chance of cell wall opening is increased in the case where there is not a high degree of branching to prevent cell opening, and therefore the expansion ratio increases. Second, if the viscosity is too high, then the expansion ratio is decreased because of too high resistance in the cell wall. If this is the case, a decreased viscosity results in an increased expansion ratio. It can be said that the content of talc does not clearly play an important role on the expansion behavior of foamed samples, and the expansion ratio increased dramatically when small amounts of talc particles were introduced into the polymer melt especially at 5 wt% CO_2. In this experiment, the optimum expansion ratio (14 folds) was obtained with 0.8 wt% talc.

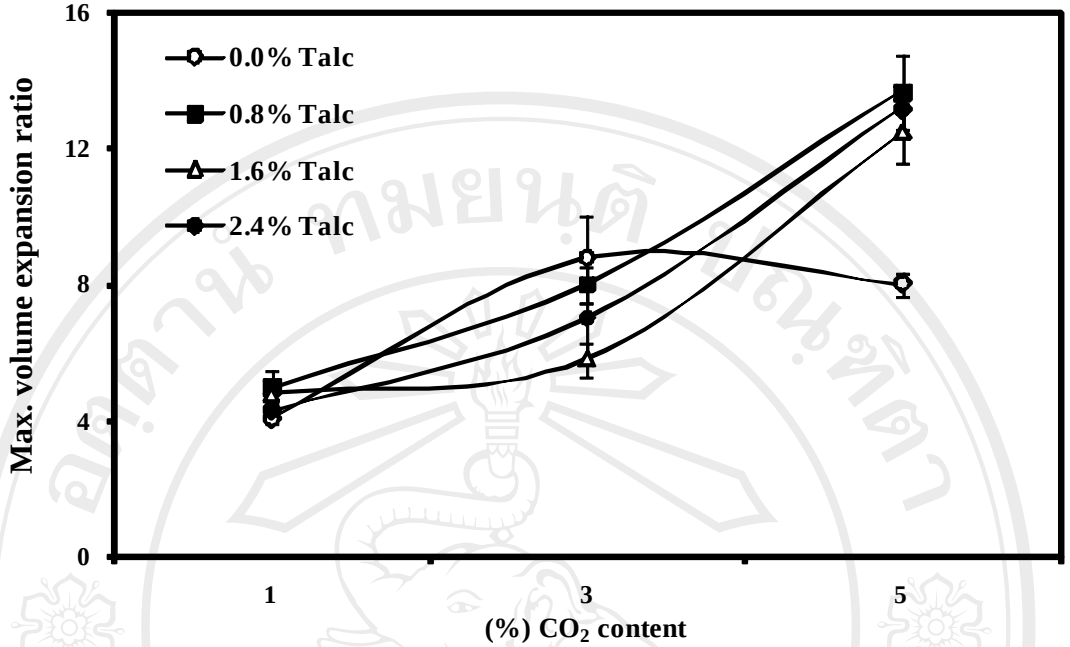

Figure 4.10 Maximum volume expansion ratios of PP foams versus CO_2 content.

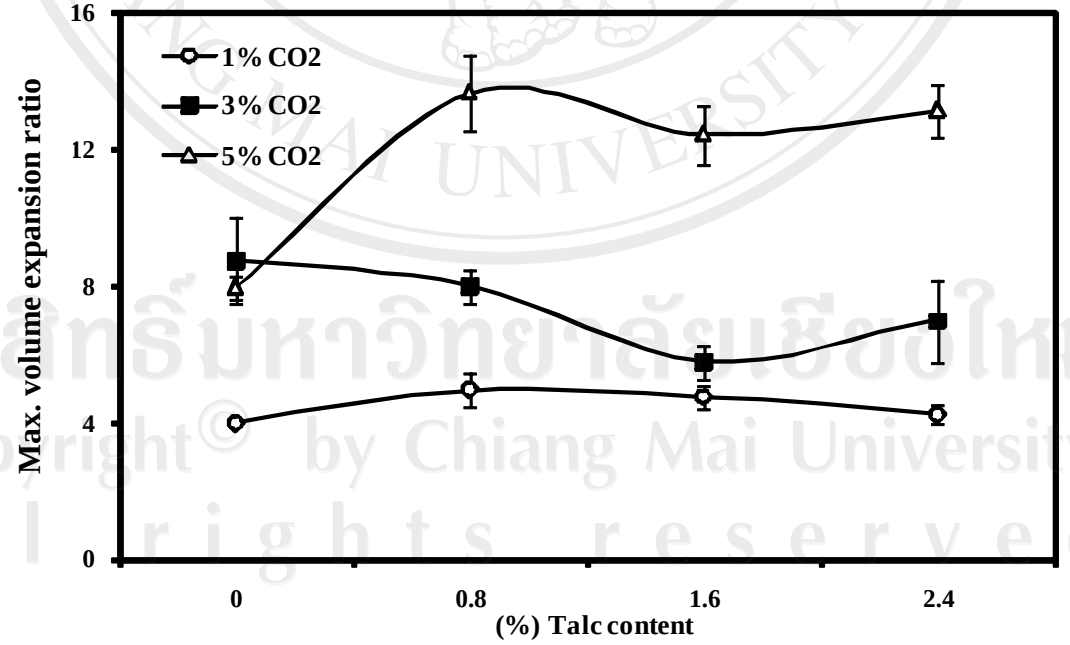

Figure 4.11 Maximum volume expansion ratios of PP foams versus talc content.

In addition, the blowing agent (CO_2) efficiency was plotted against die temperature as shown in Figure 4.12-4.15. At a high foaming temperature range (i.e., higher than 155 °C), the CO_2 efficiencies of 1 wt% at all talc contents were higher than those of 3 and 5 wt%. The maximum blowing agent efficiencies at 1 wt% CO_2 experiments were 58, 70, 68, and 60% for 0.0, 0.8, 1.6, and 2.4 wt% of talc, respectively. The CO_2 efficiency with 0.8 wt% talc was the highest. At low temperatures, the CO_2 efficiencies of 5 wt% CO_2 experiments could reach up to 40% due to the effective prevention of gas loss.

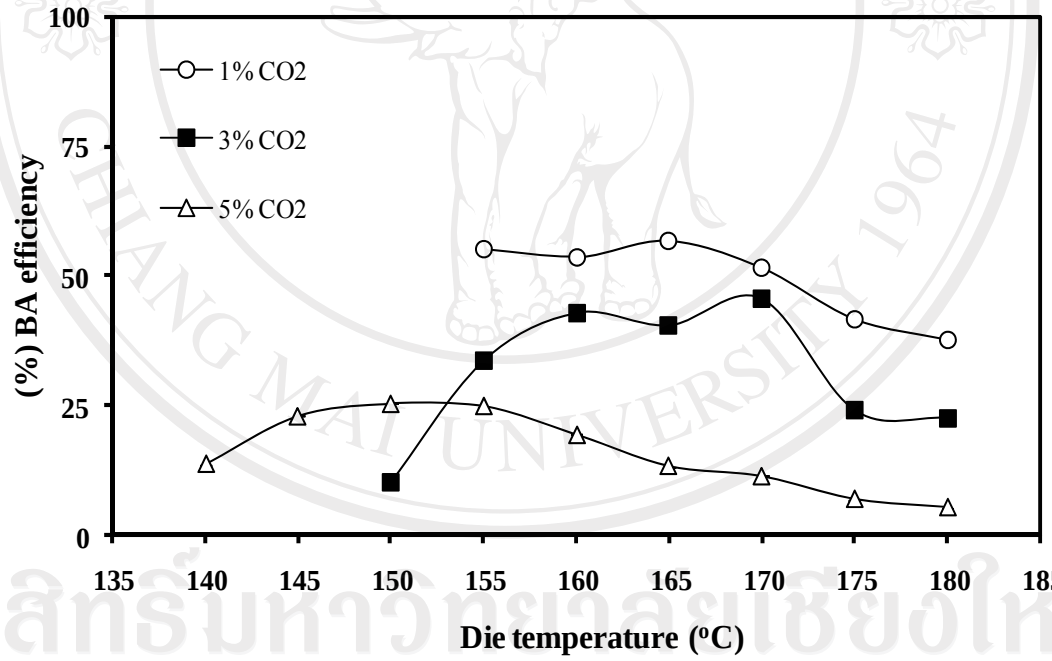

Figure 4.12 Blowing agent efficiency of PP foams with 1, 3, and 5 wt% of CO_2 without talc at various die temperatures.

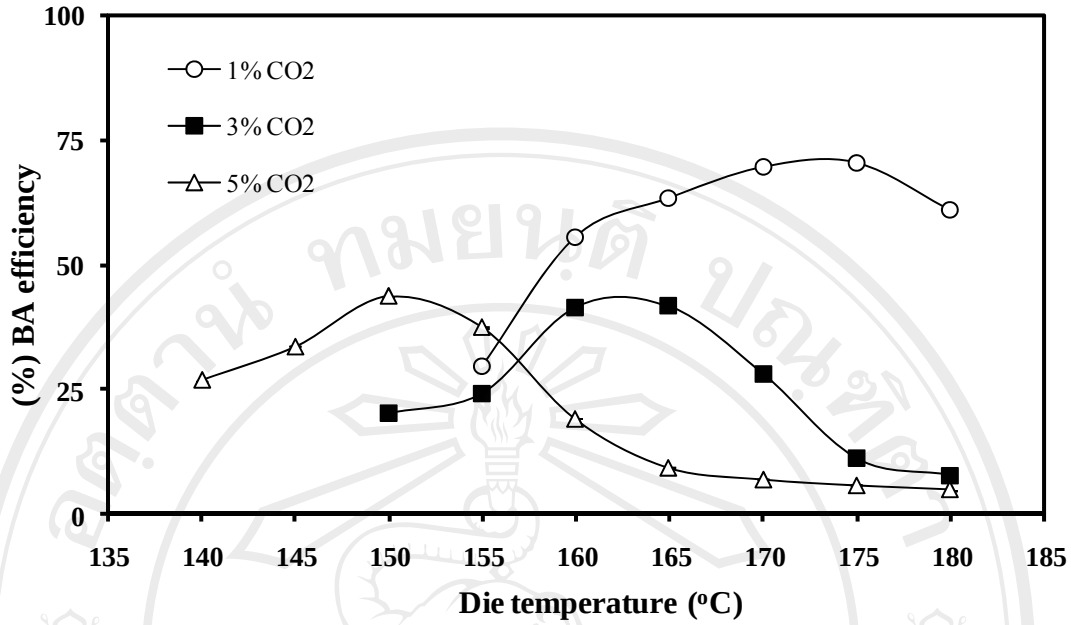

Figure 4.13 Blowing agent efficiency of PP foams with 1, 3, and 5 wt% of CO_2 with 0.8 wt% of talc at various die temperatures.

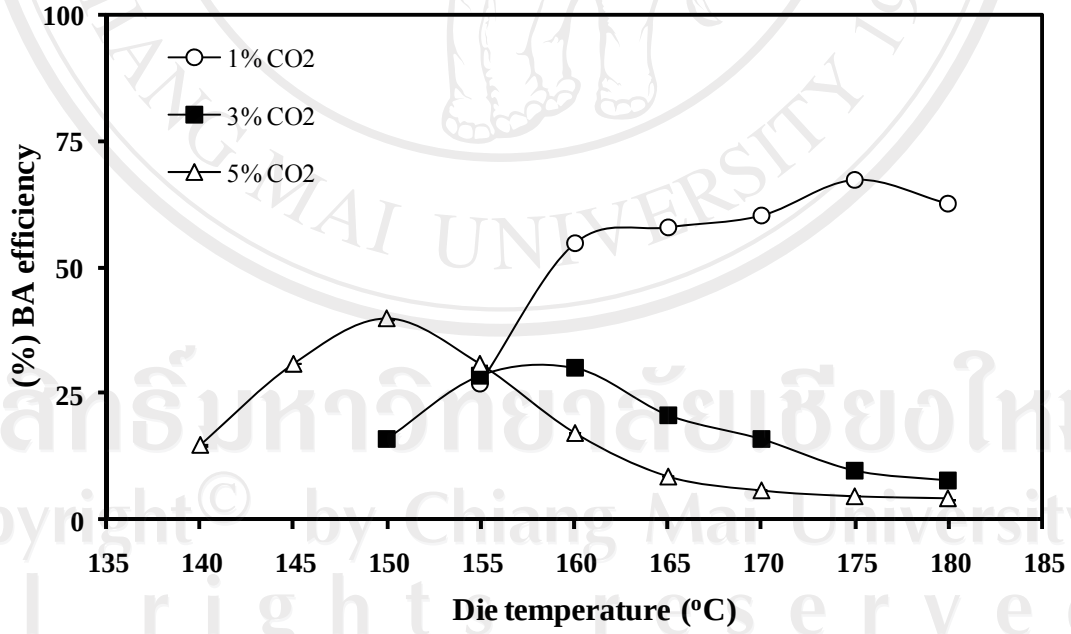

Figure 4.14 Blowing agent efficiency of PP foams with 1, 3, and 5 wt% of CO_2 with 1.6 wt% of talc at various die temperatures.

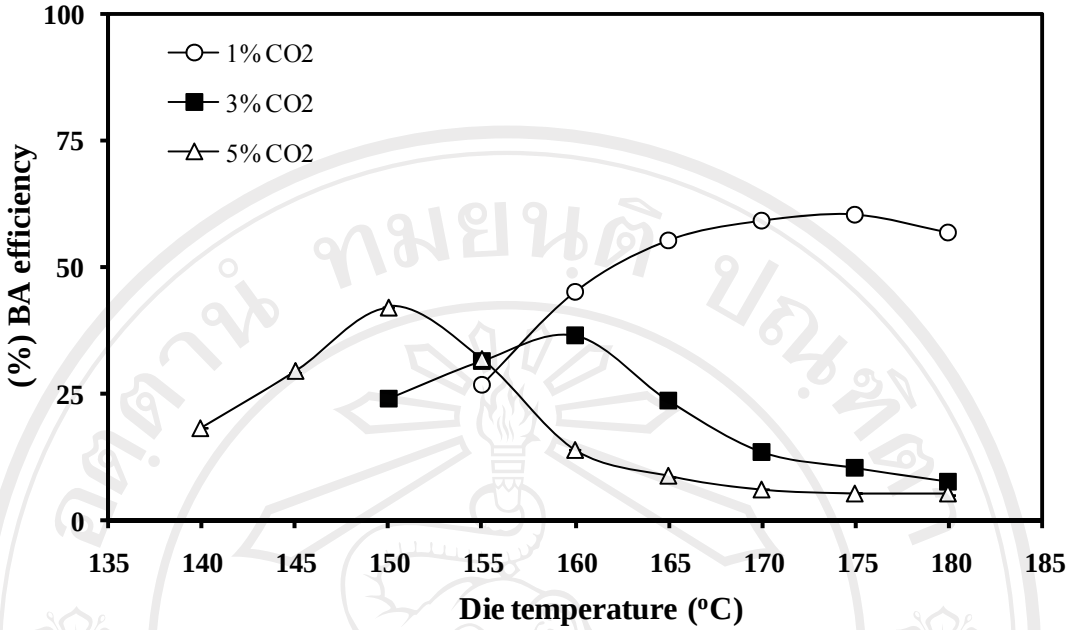

Figure 4.15 Blowing agent efficiency of PP foams with 1, 3, and 5 wt% of CO_2 with 2.4 wt% of talc at various die temperatures.

Even though the expansion ratio increased as CO_2 content increased, the gas efficiency decreased [143]. This may be due to the enhancement of gas loss caused by the increasing of plasticizing effect. The free volume increased as the viscosity of the molten polymer dropped when CO_2 was dissolved in the polymer matrix. This effect increased as the amount of gas increased; likewise, the diffusivity of CO_2 in the swollen polymer matrix must increase as well. Therefore, the chance of gas loss through the foam skin increased at a high content of CO_2.

Subsequently, the blowing agent efficiency would be lowered by foaming with a large amount of CO_2. This decreased efficiency phenomena at high content of gas implied that there would be a practical limit to the accomplishment of a high volume expansion ratio by enhancing and dissolving a large flow rate of CO_2. In addition, if the amount of CO_2 exceeds the solubility, injected CO_2 cannot completely

dissolve in the matrix, and a much lower blowing agent efficiency would be achieved [143].

4.5.5 Effects of processing parameters on cell nucleation

The cell morphology and cell density were summarized as shown in Figure 4.16-4.26, respectively. These results were discussed as the aspects of the relationship between cellular characteristics and processing conditions as following;

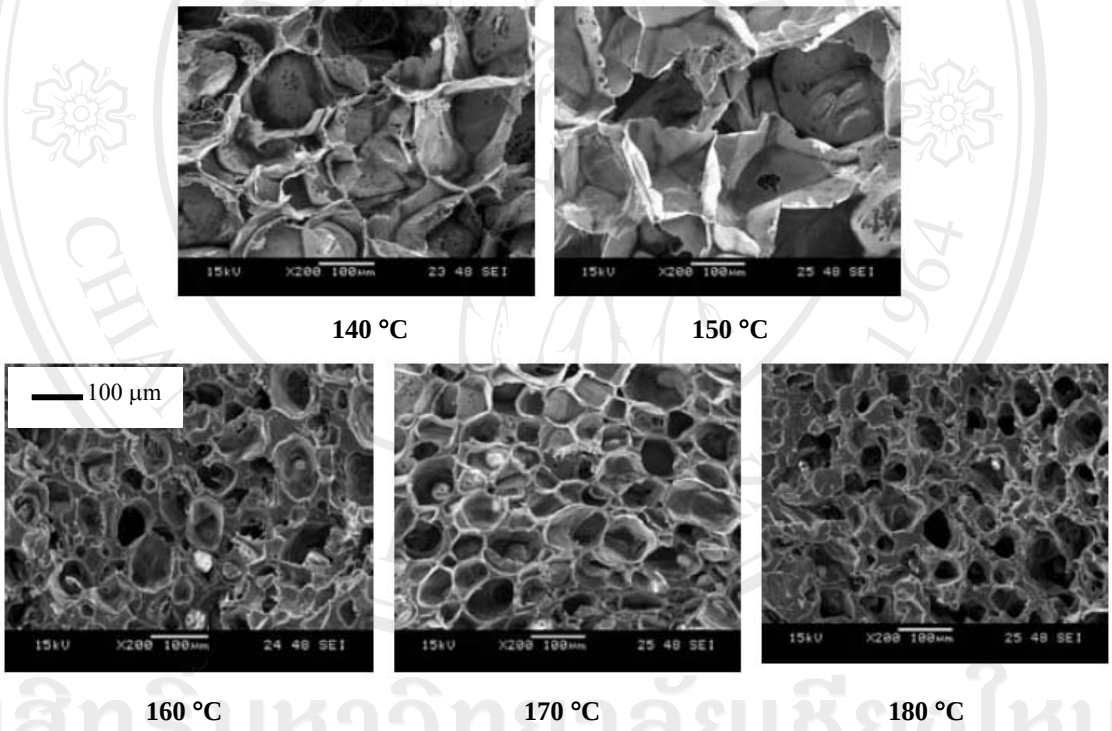

Figure 4.16 SEM images (at 200 times of magnification) of PP foams with 0.8 wt% of talc and 5 wt% of CO_2 at various die temperatures.

1) Die temperature

Figures 4.17-4.20 show the cell density of foamed samples with various CO_2 and talc contents. The cell density was insensitive to die temperatures; especially

at high temperature, cell density was maintained high. This is due to the material having a high degree of branching to prevent cell coalescence. Cell densities of this material were in general 10^7-10^9 cells/cm^3 with this filamentary die. It can be concluded that the processing temperature did not significantly influence cell nucleation of foamed samples.

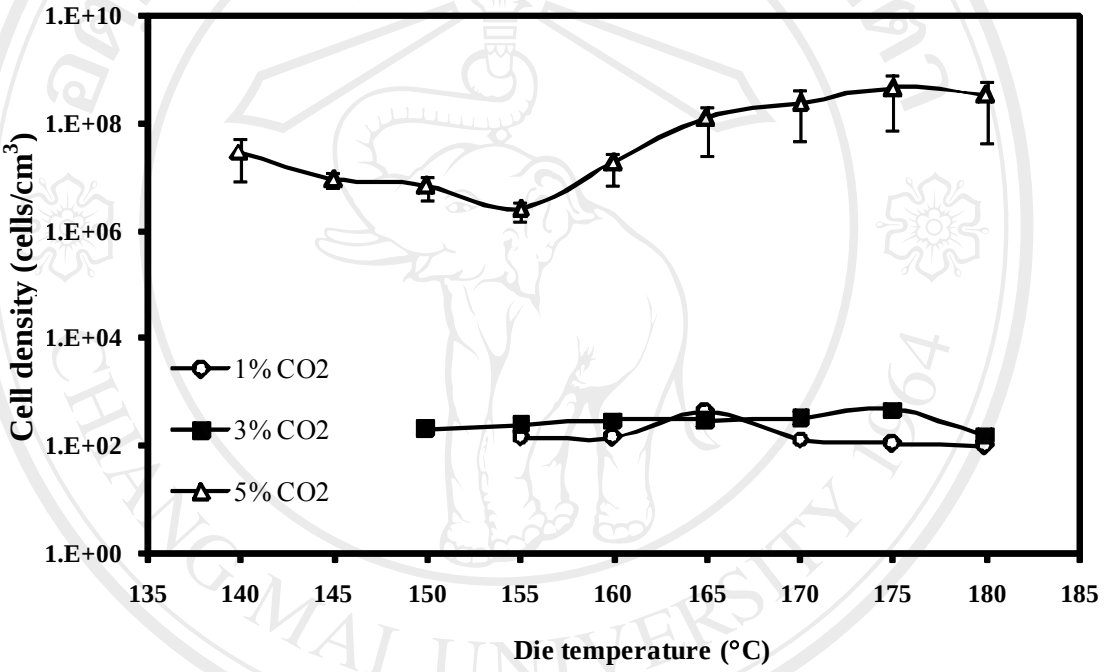

Figure 4.17 Cell densities of PP foams with 1, 3, and 5 wt% of CO_2 and without talc at various die temperatures.

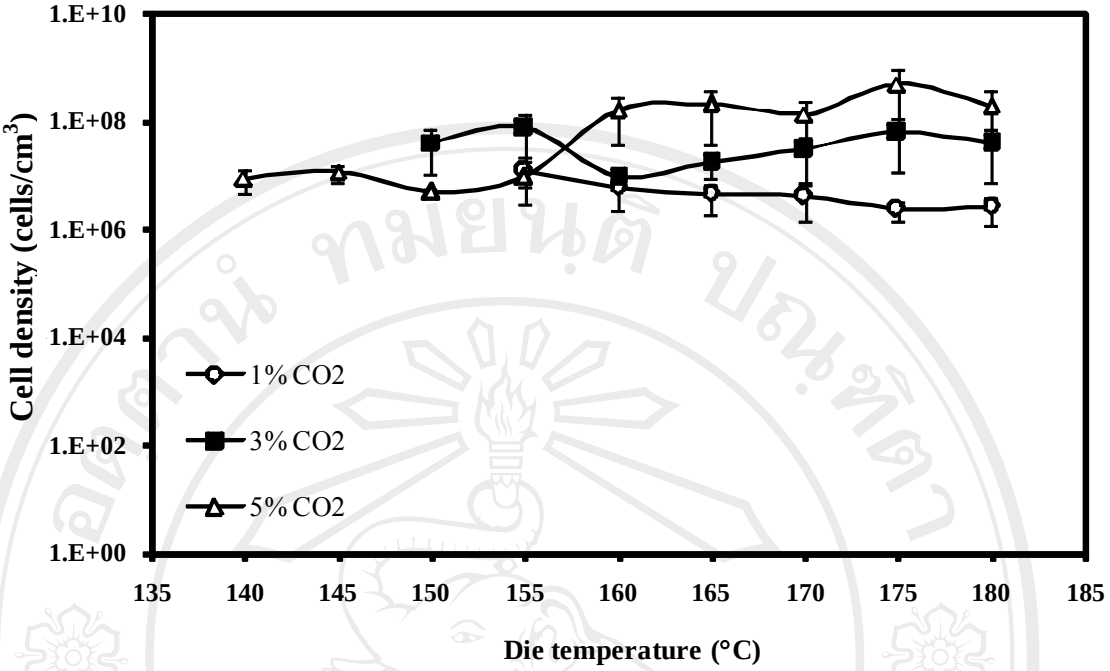

Figure 4.18 Cell densities of PP foams with 1, 3, and 5 wt% of CO_2 with 0.8 wt% of talc at various die temperatures.

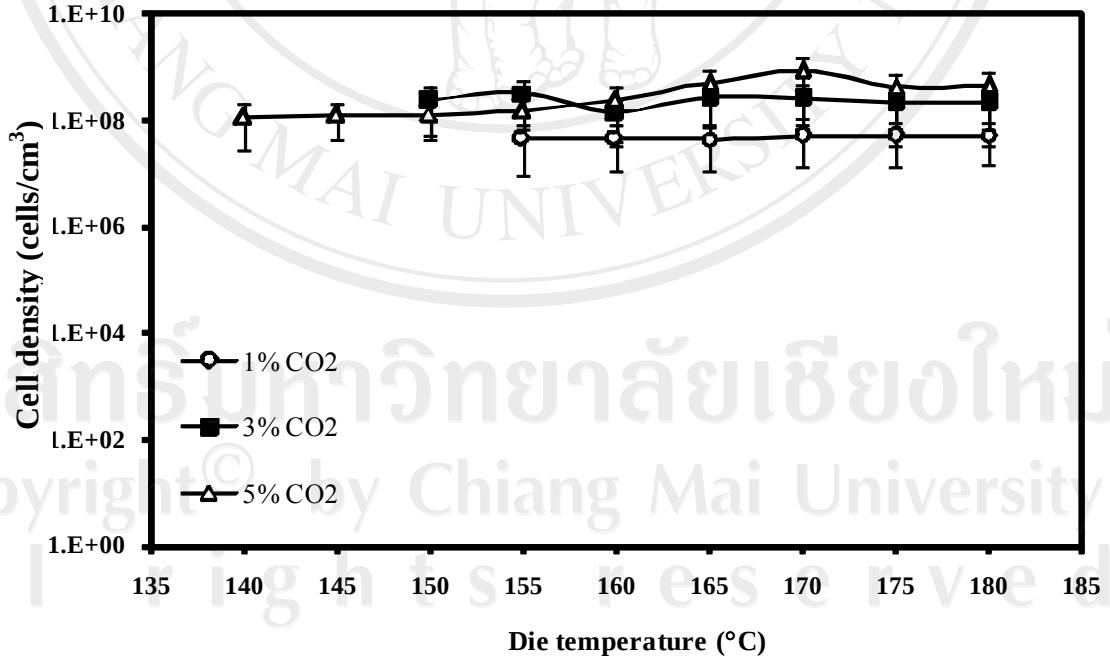

Figure 4.19 Cell densities of PP foams with 1, 3, and 5 wt% of CO_2 with 1.6 wt% of talc at various die temperatures.

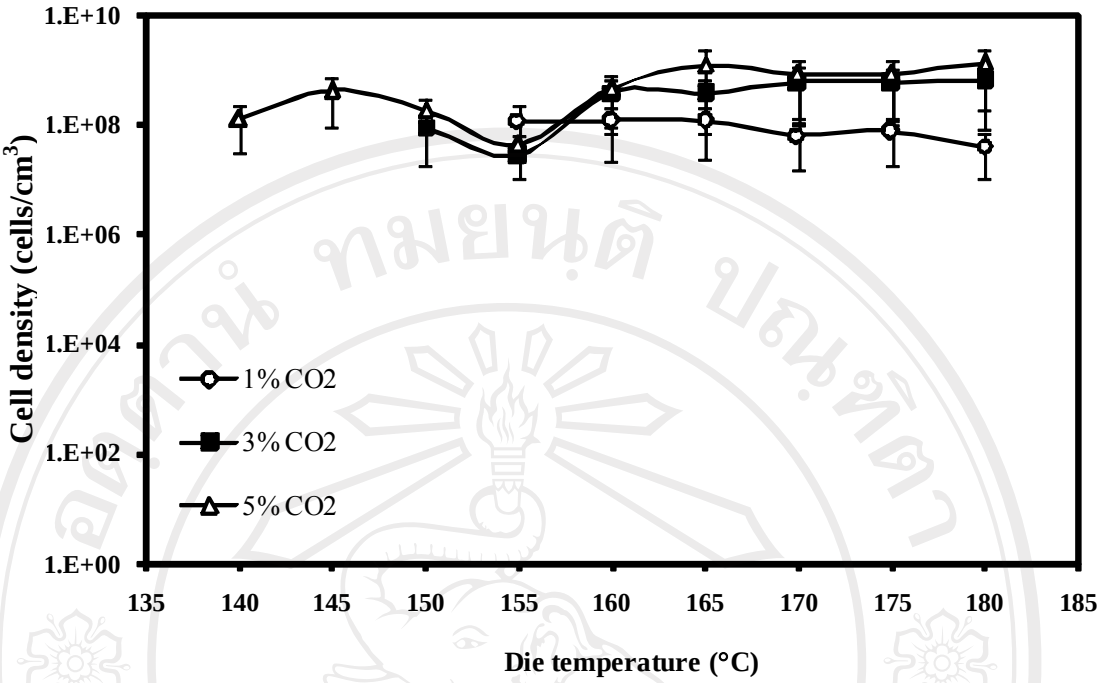

Figure 4.20 Cell densities of PP foams with 1, 3, and 5 wt% of CO_2 with 2.4 wt% of talc at various die temperatures.

2) Blowing agent content

Cell densities were significantly affected by the blowing agent content. For all talc contents, cell densities increased as CO_2 contents increased. Cell density was dramatically increased from 10^2-10^3 cells/cm^3 (i.e., five orders of magnitude) as CO_2 content was increased from 1 to 5 wt% without talc (Figure 4.21).

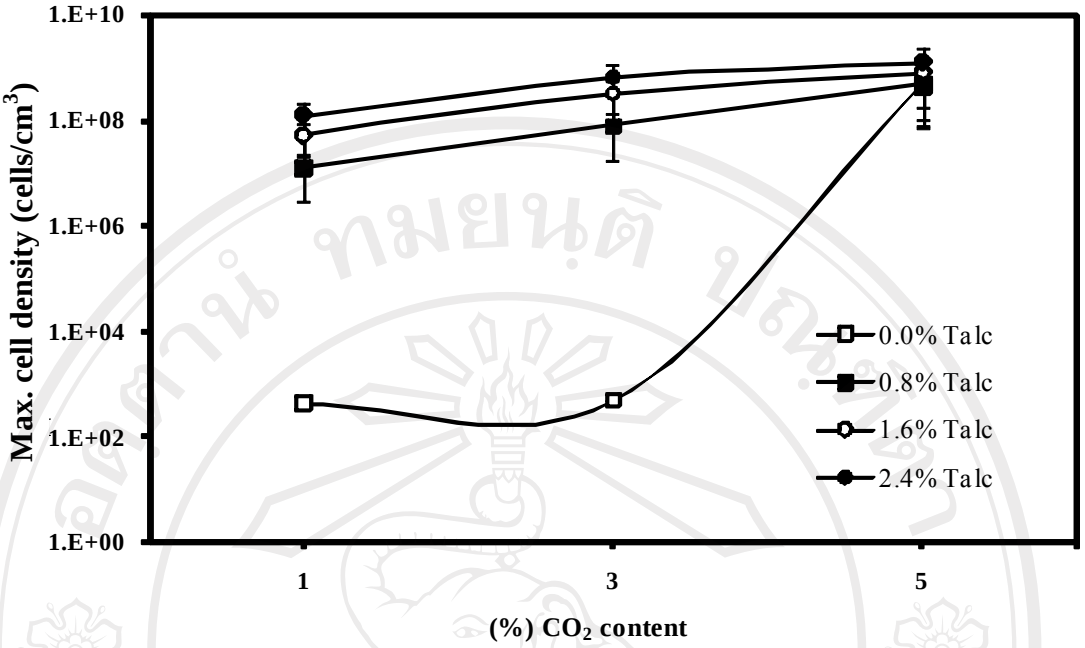

Figure 4.21 Maximum cell densities of PP foams versus CO_2 content.

However, at above 0.8 wt% talc, even though the cell densities increased gradually with the increase in talc content, the degree of improvement in cell density was less. This was also reflected in the cell size; the decrease in cell size was not significant. Therefore, when talc particles were introduced into the system, the effect of CO_2 content was less significant on cell density and cell size.

3) Nucleating agent content

When 5 wt% CO_2 was used, added talc did not affect the number of cells and bubble size. This indicates that the addition of talc was very effective for nucleation when foaming with CO_2 at low contents (1 and 3 wt%), but it did not play a significant role on cell nucleation at high contents of CO_2 as shown in Figure 4.21-

4.22, which shows the plot of cell density as a function of CO_2 and talc contents, respectively.

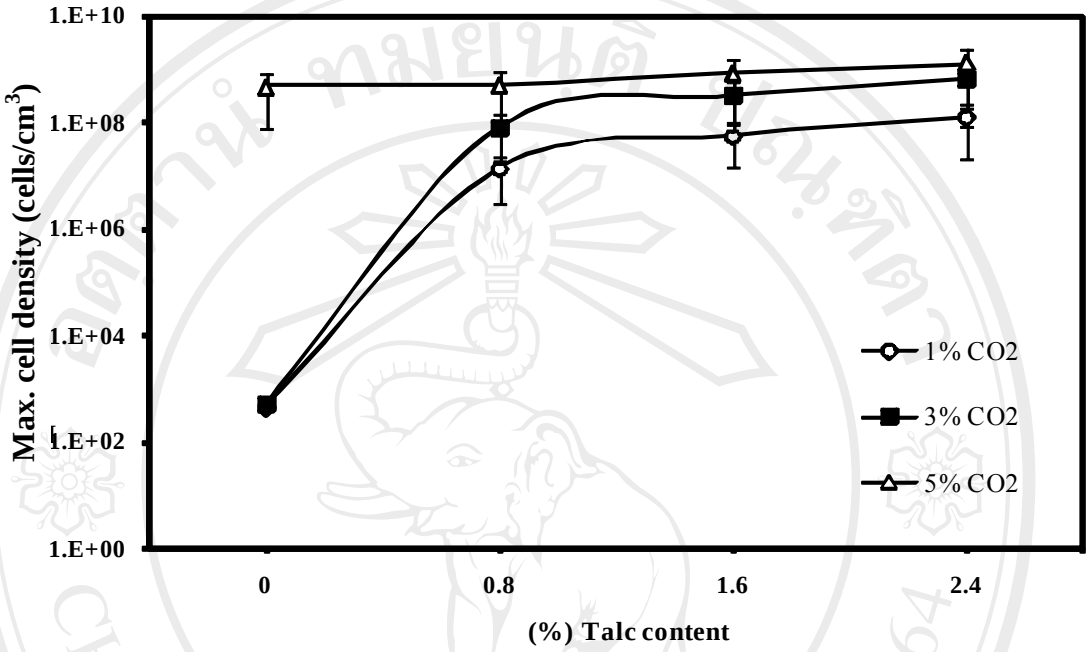

Figure 4.22 Maximum cell densities of PP foams versus talc content.

Therefore, it may be concluded that at low CO_2 and talc contents, cell density was strongly affected by both CO_2 and talc. When either CO_2 or talc content was high, cell nucleation was governed by the high concentration of one agent regardless of the content of the other. Again, from the results in Figure 4.22, it was also observed that the cell density tended to initially level off at 0.8 wt% talc concentration. The addition of talc content above 1.6 wt% did not improve the cell density and cell size because of the possible agglomeration of talc particles. A slightly increase in cell density was achieved with the increase in talc content. This means that excessive talc particles will be agglomerated while retaining the number of effective nucleation sites. Cell nucleation was not a function of die temperature, while it was

affected by small talc concentration and high CO_2 content. Moreover, a large number of cells, up to 10^7-10^9 cells/cm^3 and fine cells (i.e., less than 0.02 mm), was easily achieved in all combinations with talc particles as shown in Figure 4.23-4.26.

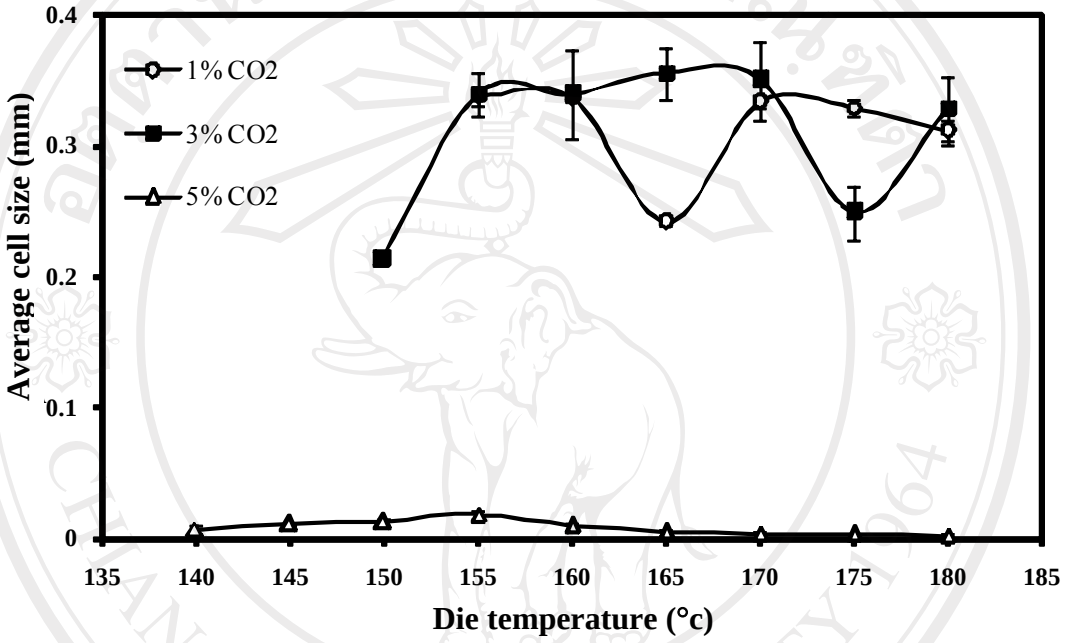

Figure 4.23 Average cell size of PP foams with 1, 3, and 5 wt% of CO_2 without talc at various die temperatures.

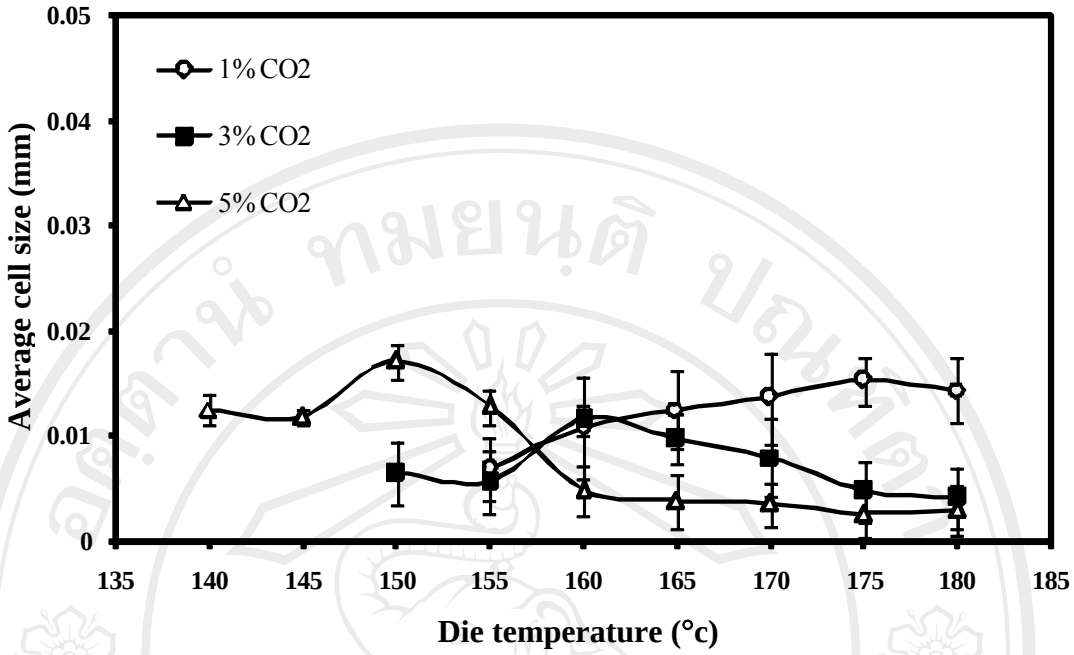

Figure 4.24 Average cell size of PP foams with 1, 3, and 5 wt% of CO_2 with 0.8 wt% of talc content at various die temperatures.

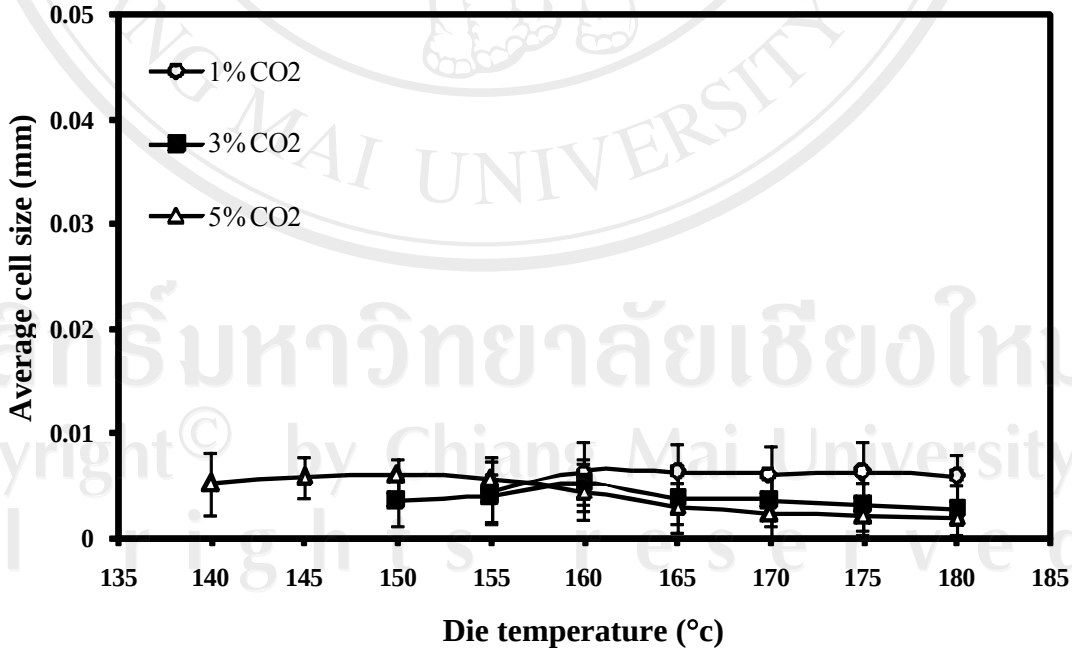

Figure 4.25 Average cell size of PP foams with 1, 3, and 5 wt% of CO_2 with 1.6 wt% of talc content at various die temperatures.

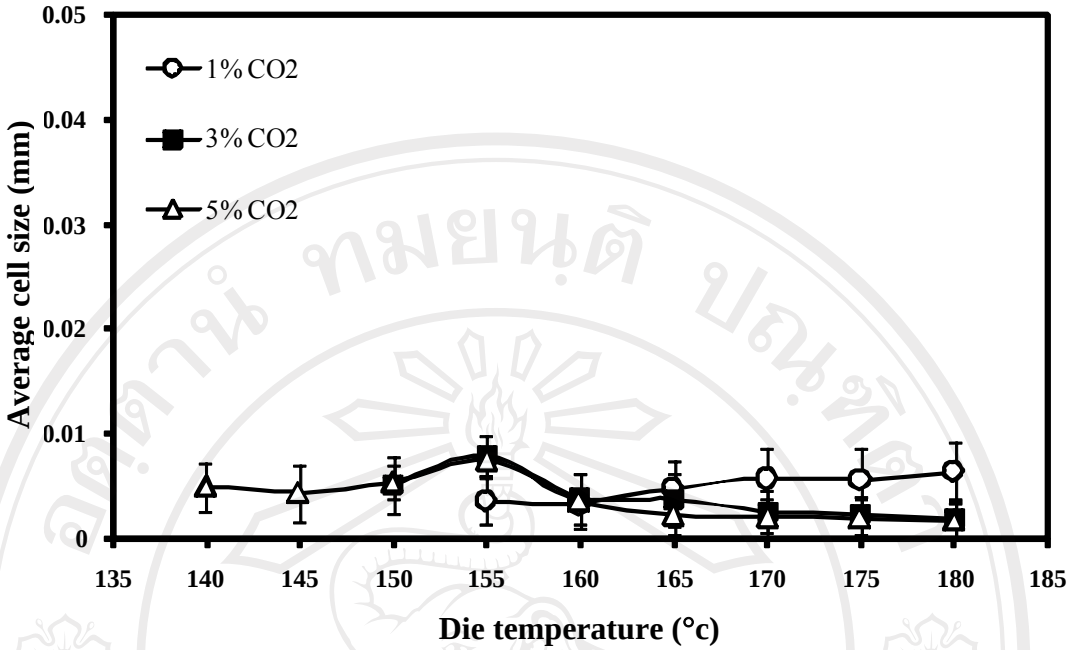

Figure 4.26 Average cell size of PP foams with 1, 3, and 5 wt% of CO_2 with 2.4 wt% of talc content at various die temperatures.

4.6 Conclusions

In this study, low density, fine-celled PP foams were successfully produced by using a recyclable HMS branched PP resin as a polymeric matrix to suppress cell coalescence. A filamentary die was selected to promote the optimum pressure and pressure drop rate at various die temperatures. CO_2 and talc were utilized as a blowing agent and a nucleating agent, respectively. The effects of varying CO_2 and talc contents on volume expansion and cell nucleation behaviors were investigated. The expansion behavior was governed by two mechanisms; at high temperatures, the gas loss phenomenon affected the expansion behavior of foams. At lower temperatures, crystallization of the polymer was the dominating factor on the expansion behavior. These phenomena were very clearly observed at high CO_2 contents (i.e., 3 and 5 wt%). Optimum temperatures tended to shift to lower

temperatures because of the plasticization effect with the increased CO_2 content. The expansion behavior was not clear at 1 wt% CO_2 for all talc contents, and the maximum expansion ratio was only 4-6 folds. Expansion ratios increased as CO_2 content increased, and the expansion ratios showed the mountain shaped curves. The maximum expansion ratio up to 12-14 folds was successfully obtained at 0.8 wt% talc with 5 wt% CO_2. On the other hand, the blowing agent efficiency did not increase proportionally to the increase in CO_2 content. The maximum blowing agent efficiency of 70% was achieved at 0.8 wt% talc with 1 wt% CO_2. The CO_2 content played an important role on the cell nucleation behavior when foaming this polymer without talc particles. The cell density was noticeably increased as the CO_2 content was increased to 5 wt% while the bubble size decreased. The maximum number of cells, up to 10^7-10^9 cells/cm^3 and small cells (less than 0.02 mm), were easily achieved in this experiment. On the other hand, talc content showed obvious changes in cell density and cell size when foaming with small amount of CO_2 (i.e., 1 and 3 wt%). But the maximum expansion ratio seemed to decrease slightly as the talc content was increased. This could be due to one of two reasons: (1) this polymer had a low degree of branching and (2) its viscosity was too high. If these were the cases, an increase in the degree of branching and a decrease in viscosity would result in increased expansion ratio. However, the expansion ratios of up to 14-fold and cell densities of up to 10^7-10^9 cells/cm^3 were successfully achieved when using 0.8 wt% talc with 5 wt% CO_2 in the tandem foaming extrusion system.